analytical chemistry

ARTICLE

pubs.acs.org/ac

Droplet-Based Pyrosequencing Using Digital Microfluidics

Deborah J. Boles,[†] Jonathan L. Benton,[†] Germaine J. Siew,[†] Miriam H. Levy,[†] Prasanna K. Thwar,[†] Melissa A. Sandahl,[†] Jeremy L. Rouse,[†] Lisa C. Perkins,[†] Arjun P. Sudarsan,[†] Roxana Jalili,[§] Vamsee K. Pamula,[†] Vijay Srinivasan,[†] Richard B. Fair,[‡] Peter B. Griffin,[§] Allen E. Eckhardt,[†] and Michael G. Pollack*[,†]

[†]Advanced Liquid Logic Incorporated, Research Triangle Park, North Carolina, United States

[‡]Department of Electrical and Computer Engineering, Duke University, Durham, North Carolina, United States

[§]Stanford Genome Technology Center, Stanford University, Palo Alto, California, United States

Supporting Information

ABSTRACT: The feasibility of implementing pyrosequencing chemistry within droplets using electrowetting-based digital microfluidics is reported. An array of electrodes patterned on a printed-circuit board was used to control the formation, transportation, merging, mixing, and splitting of submicroliter-sized droplets contained within an oil-filled chamber. A three-enzyme pyrosequencing protocol was implemented in which individual droplets contained enzymes, deoxyribonucleotide triphosphates (dNTPs), and DNA templates. The DNA templates were anchored to magnetic beads which enabled them to be thoroughly washed between nucleotide additions. Reagents and protocols were optimized to maximize signal over background, linearity of response, cycle efficiency, and wash efficiency. As an initial demonstration of feasibility, a portion of a 229 bp *Candida parapsilosis* template was sequenced using both a de novo protocol and a resequencing protocol. The resequencing protocol generated over 60 bp of sequence with 100% sequence accuracy based on raw pyrogram levels. Excellent linearity was observed for all of the homopolymers (two, three, or four nucleotides) contained in the *C. parapsilosis* sequence. With improvements in microfluidic design it is expected that longer reads, higher throughput, and improved process integration (i.e., "sample-to-sequence" capability) could eventually be achieved using this low-cost platform.

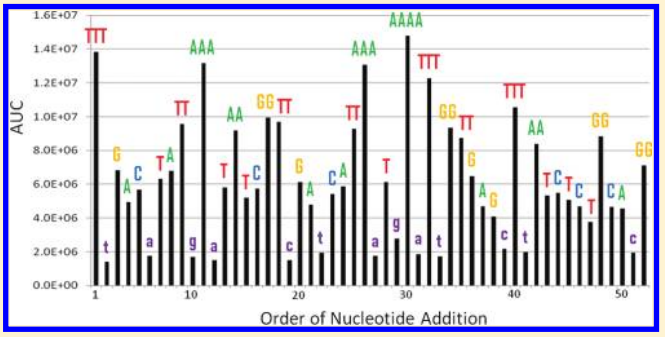

Since the completion of the human genome project in 2003, an impressive array of new technologies has been developed and applied to DNA sequencing resulting in massive improvements in throughput and cost. DNA sequencing has now advanced to the point where the sequencing of whole genomes is routine and the ambitious goal of sequencing individual human genomes for less than $1 000 is likely to be achieved within the next several years.[1] As both the quantity of sequence and the ability to interpret it increases, new applications of DNA sequencing are rapidly emerging. Examples include the use of sequencing to analyze transcriptomes (RNA seq), protein−DNA interactions (ChIP seq), epigenomics, metagenomics, and copy number variation. Each sequencing technology has characteristic strengths and weaknesses which determine its suitability for a particular application. As applications become increasingly diverse and specialized it is likely that no single sequencing platform will be able accommodate all needs. Even a single platform may be offered in multiple different formats to meet the specific needs of various applications, use environments, and workflows. This is evident in the recent trend among the major sequencing instrument providers to offer lower throughput versions of their instruments which are smaller, less expensive, and with more integrated workflows for use by individual researchers.

Pyrosequencing is a sequencing-by-synthesis method which is currently employed in several commercially available platforms. The feasibility of implementing a miniaturized version of pyrosequencing using a "digital microfluidic" lab-on-a-chip device is described here. Digital microfluidics refers to a paradigm for miniaturized liquid handling in which discrete droplets are individually and programmably manipulated using a set of basic stepwise operations.[2] One of the most common and flexible implementations of digital microfluidics is based on the use of electrowetting arrays to manipulate individual droplets.[3] The electrowetting effect provides a convenient means for controlling the wettability of a hydrophobic surface through the application of electrical fields at the solid−liquid interface.[4] A typical electrowetting-based digital microfluidic device includes a substrate carrying an array of insulated surface electrodes which is opposed by another plate to form an enclosed chamber in which the droplets are electrically manipulated. Both surfaces of the chamber are coated with a hydrophobic material, and the remaining space is filled by either air or an immiscible fluid

Received: June 10, 2011
Accepted: September 20, 2011
Published: September 20, 2011

such as silicone oil to prevent evaporation of the droplets. Basic operations such as dispensing, transporting, merging, and splitting of individual droplets are controlled by specific sequences of voltage activation of the electrode array.[5,6] Complex, multistep assays and protocols can be implemented as a series of software instructions linking these basic droplet operations together. Several useful applications in chemistry and biology have previously been developed using this versatile microfluidic platform including real-time polymerase chain reaction (PCR),[7] immunoassays,[8] clinical chemistry,[9] cell culture,[10] and sample preparation.[11] Applications of digital microfluidics in chemistry and biology[12,13] as well as in clinical diagnostics[14] have recently been reviewed elsewhere.

In pyrosequencing, individual nucleotide bases are added in succession to a primed DNA template in the presence of DNA polymerase.[15] The addition of a nucleotide which is complementary to the next unpaired base results in the incorporation of that nucleotide into the synthesized strand with the concomitant release of inorganic pyrophosphate (PPi) molecules equivalent to the number of nucleotide bases incorporated. ATP sulfurylase converts pyrophosphate to ATP which drives the oxidation of luciferin by luciferase, resulting in a visible light product. Quantitative chemiluminescent detection of pyrophosphate is used as a basis to detect an incorporation event and to estimate the number of bases incorporated into the synthesized strand of DNA. Apyrase is typically used to degrade ATP and unincorporated nucleotides prior to the next round of nucleotide addition. These four enzymatic reactions (nucleotide incorporation, ATP production, light generation, and nucleotide degradation) are usually performed as a "single-pot" reaction but, in principle, could be performed as a series of sequentially separated reactions. Washing can also be used in place of apyrase or as an adjunct to apyrase to remove nucleotides as well as other reaction byproducts. The three-enzyme system adapted in this report excludes apyrase and therefore requires efficient washing between each cycle of nucleotide addition. Since its introduction about 20 years ago[16−18] the pyrosequencing technique has now been refined, automated and scaled[19] to the point where commercial high-throughput systems such as the GS-FLX (Roche/454) have been used for whole-genome sequencing and can generate average read lengths of >400 bp and >500 Mb of sequence data in a single run. Other systems such as the PyroMark (Qiagen/Biotage) have been commercialized for specialized low-throughput applications such as pathogen identification, mutation detection, and methylation analysis. Both of these commercial products are built upon complex liquid handling systems which impose disadvantages with respect to size, cost, and portability.

Several research groups have attempted to improve upon the performance, cost, and automation of these systems by adapting pyrosequencing to miniaturized formats. Zhou et al.[20] demonstrated a microfluidic device for pyrosequencing in which deoxyribonucleotide triphosphates (dNTPs) were injected through microcapillaries into a microchamber containing the DNA to be sequenced. However, both the read length and the ability to sequence through homopolymers were severely limited due to dilution effects. Russom et al.[21] demonstrated a proof-of-concept for pyrosequencing of DNA immobilized on beads in a channel-based microfluidic device. The beads were retained within a 50 nL chamber by a filter, and reagents and wash buffer were flowed through the chamber enabling a single-nucleotide polymorphism to be successfully scored. Compared to these continuous-flow approaches the implementation of pyrosequencing in a droplet-based format offers several potential advantages including (i) the confinement of reactants within droplets prevents the dilution of reaction products, minimizes reagent consumption, and enables rapid fluid exchange, (ii) multiple sequencing reactions can be performed in parallel with independent conditions (e.g., order of nucleotides) for each reaction, (iii) enzymatic reactions including DNA polymerization, ATP production, and light generation can be segregated into separate droplets enabling reaction conditions and kinetics to be separately optimized and enabling the reactions to be separated in time and position. From an operational perspective pyrosequencing is essentially a series of repeated liquid handling steps. Because digital microfluidics enables very rapid and precise automated liquid handling it is naturally amenable to the pyrosequencing process as demonstrated in this report.

EXPERIMENTAL SECTION

Digital Microfluidic Cartridge. The digital microfluidic cartridge (Figure 1A) was constructed by bonding together a bottom plate containing the electrical features and a top plate containing sample and reagent wells. The bottom plate (127.7 mm × 85.5 mm, 0.8 mm thickness) containing the electrodes and the contact pads was fabricated using a standard printed circuit board (PCB) process, laminated with a polyimide dielectric film, and then coated with a thin hydrophobic coating. The individual electrodes comprising the electrode network were square in shape and positioned on a square grid with 1.125 mm pitch. An array of 108 contact pads on one end of the PCB was used to provide electrical connections between the cartridge and the controller instrument. The top plate was composed of either a single piece of injection-molded polycarbonate (PC) or an injection-molded PC plate attached to the top side of a glass plate with holes drilled in it. The interior surface of the top plate was coated with a transparent conductive coating and a thin hydrophobic coating. The chamber height was approximately 275 μm which in combination with the 1.125 mm electrode pitch defined a single-sized droplet with a nominal volume of 350 nL. For convenience and clarity, nominal droplet volumes of 350 nL for a single-electrode-sized droplet, 700 nL for a double-electrode-sized droplet, and so forth are used in this report although the actual volumes were not measured and could have deviated from these values.

Cartridge Controller Instrument. The cartridge was operated using a custom-built benchtop instrument incorporating all of the required control and detection capabilities (Figure 1B). The instrument contained electronics for delivering actuation voltages to the electrodes as well as detection electronics. The device was operated by applying a 300 V potential between the top plate reference electrode and the insulated control electrodes on the PCB surface. Although the voltages were DC, the polarity was reversed 30 times/s to prevent any charging effects. Instrument functions were controlled by an embedded microprocessor which was capable of storing and executing programs out of an on-board memory. The instrument was linked to a personal computer through a USB interface to enable the exchange of command signals, programs, and data. The cartridge was situated within a deck of machined aluminum which provided alignment to the magnets, the optical detector, and the spring-loaded electrical connector pins. Rectangular (1/4 in. × 1/8 in. × 1/16 in.) neodymium magnets (no. B421, K&J Magnetics) were inserted within the deck at locations intended for the manipulation of paramagnetic beads. The stationary magnets were embedded within a machined plastic insert fitted into the aluminum deck which oriented them under the detector (position 1). The insert

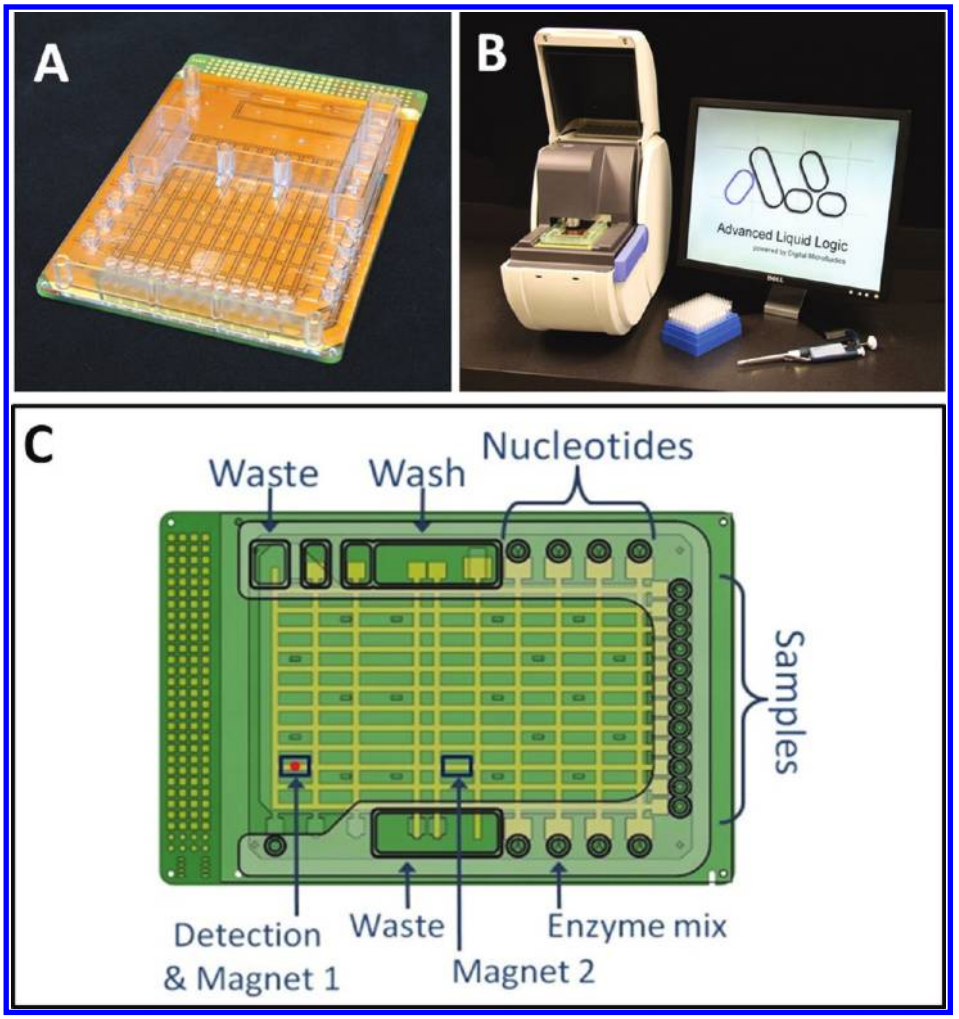

Figure 1. (A) Photograph of the assembled multiwell-plate-sized PCB-based cartridge, (B) photograph of the sequencing instrument, and (C) schematic illustration of the cartridge showing locations of sample and reagent wells and other features.

could also be removed and rotated 180° between experiments to relocate them to the center of the cartridge (position 2). Luminescent detection was achieved using a photon-counting photomultiplier tube (PMT) module (H7155, Hamamatsu, Japan) coupled to a custom optical assembly which was mounted above the deck. The optics consisted of a set of three lenses designed to collect the light from a specific location on the cartridge corresponding to the detection electrode. A 2.2 mm aperture was inserted into the optical path at the PMT sensor to reduce the light signal to within the linear range of the PMT module.

PCR Amplification and Preparation of *Candida parapsilosis* Templates. A 229 bp fragment was amplified from *C. parapsilosis* genomic DNA purified from culture using forward and reverse primers targeting the ITS1 and ITS2 regions (additional details in the Supporting Information). The PCR product was purified using a PCR purification kit (QIAquick, Qiagen, Germany) and verified by gel electrophoresis. The PCR product was then bound to magnetic beads and prepared for sequencing as follows. An amount of 100 μL of streptavidin M280 Dynabeads (Life Technologies, Carlsbad, CA) was washed three times and resuspended in 100 μL of 2× binding buffer (10 mM Tris pH 7.6, 2 M NaCl, 1 mM EDTA, 0.1% Tween 20). Amounts of 3−5 μg of biotinylated PCR amplicon in 100 μL of H_2O were added to the beads, and they were incubated at 65 °C for 15 min with periodic mixing. The double-stranded amplicon was denatured by incubating the beads in 100 μL of 0.5 M NaOH for 1 min. The beads were washed once in NaOH followed by three additional washes in magnesium annealing buffer (20 mM Tris acetate, pH 7.6, 5 mM magnesium acetate). The beads were resuspended in 100 μL of magnesium annealing buffer prior to adding 5 μL of 10 μM sequencing primer, 5′-aagagatccRttgttRaaagt-3′. The solution was heated to 80 °C for 2 min and allowed to cool back down to room temperature in the heat block. The bead/template/primer complex was washed three times in pyrosequencing wash buffer as described below; then 15−20 μg of single-stranded binding protein (SSB) (Affymetrix, Santa Clara, CA) was added, and the mixture was incubated at room temperature for 10 min. The beads were washed with pyrosequencing wash buffer and resuspended in 200 μL of pyrosequencing wash buffer to achieve a final concentration of 5 μg/μL of beads. On the basis of the manufacturer's specified binding capacity it is estimated that the 700 nL aliquot used in each sequencing reaction contained between 150 and 460 fmol of template DNA.

Reagent Preparation for Targeted and de Novo Pyrosequencing. Separate stock solutions were prepared for pyrosequencing wash buffer, enzymes, dNTPs, and DNA. Pyrosequencing wash

dx.doi.org/10.1021/ac201416j |*Anal. Chem.* 2011, 83, 8439–8447

buffer was composed of 100 mM Tris acetate pH 7.6, 0.5 mM EDTA pH 8.0, 5 mM magnesium acetate, and 0.01% Tween 20. Enzyme solution was prepared at a 3× concentration and contained pyrosequencing wash buffer with 13.5 mU/μL ATP sulfurylase, 1.5 μg/μL luciferase, 1.8 μg/μL D-luciferin, 6.9 U/μL Klenow (exo-), and 0.02% Tween 20. Stock solutions of each dNTP were prepared at 3× concentration with 18 μM of nucleotide (dTTP, dCTP, dGTP, or dATPαS) added to pyrosequencing wash buffer with 15 μM adenosine phosphosulfate (APS), 3 mM dithiothreitol (DTT), and 120 ng/μL single-stranded binding protein (SSB). The two-step protocol in which base incorporation and signal detection were performed in separate droplets required a slight reformulation of the enzyme and dNTP stock solutions. In these experiments, the enzyme mix was prepared at a 2× concentration as described above but without the Klenow (exo-). Stock solutions of dNTPs were prepared at a 2× concentration as described above but also included 4.6 U/μL Klenow (exo-) and 20 μM APS.

Cartridge Preparation. A new microfluidic cartridge which had been stored within a vacuum-sealed bag was used for each experiment. Dry cartridges were inserted into the instrument deck and locked into place. The cartridges were then filled with approximately 2.4 mL of 2 cSt silicone oil (Gelest, Morrisville, PA) with 0.05% Span 85 (w/v). Subsequently, 6.4 μL of enzyme solution, 6.4 μL of each dNTP solution, 3.2 μL of DNA template/primer complex on magnetic beads, and 800 μL of wash buffer were each loaded into separate wells on the cartridge as illustrated in Figure 1C. Due to capacity constraints reagent wells were typically reloaded after every 10 nucleotide incorporation cycles. An automatic pause inserted into the program enabled the operator to add additional reagents without removing the cartridge or otherwise interfering with the experiment.

Fluidic Protocol for Single-Pot Reaction. Two droplets (∼350 nL each) of DNA/primer/bead complex were dispensed within the cartridge, merged together, and transported over a magnet located beneath the detection electrode (magnet 1 position). The magnetic beads were immobilized within the double-droplet and washed six times by merging a double-droplet (∼700 nL) of wash buffer with the sample, splitting off a double-droplet from the opposite side, and transporting that double-droplet to waste. After washing, a single-droplet was split-off and transported to waste resulting in a single-droplet containing the DNA/primer/bead complex at the magnet. Single droplets of dNTP and enzymes were dispensed, transported to the magnet, and merged with the DNA/primer/bead complex droplet. A background luminescence reading of the sample was taken before the addition of the enzyme and dNTP droplets. The combined (∼1050 nL) droplet was then mixed by transporting it back and forth across eight electrodes and then held underneath the detector for a 1 min detection. Photon counts were collected from the PMT every quarter second giving 240 data points for each detection cycle. With the magnetic beads immobilized, a single-droplet was split off and transported to waste and the remaining double-droplet containing the DNA/primer/bead complex was washed as described above followed by the next round of nucleotide addition. The cycle time between nucleotide additions was approximately 3.5 min which comprised 72 s for bead washing, 10 s for combining reagents with the beads, 37 s for bead collection on the magnet and preparation for washing, 31 s for droplet transport, and 60 s for reagent mixing and detection of signal. The fluidic protocols were identical for resequencing and de novo experiments except for the order in which nucleotides were added. In resequencing experiments, nucleotides were added in a defined order based on a reference sequence of the sample. Noncomplementary nucleotides (i.e., "mismatches") were occasionally inserted into the sequence to enable the determination of background signal levels throughout an experiment. In de novo sequencing experiments, nucleotides were added in a repeated cyclical pattern that did not vary throughout the experiment (e.g., A, C, G, T, A, C, G, T, ...).

Fluidic Protocol for Separation of Incorporation and Detection Reactions. Two droplets (∼350 nL each) of DNA template, primer, and bead complex were dispensed, merged together, and transported to the magnet 2 position located in the center of the cartridge. The sample was then washed six times as described above resulting in a single-droplet containing DNA/primer/bead complex at the magnet. A single-droplet containing dNTPs, Klenow (exo-), and 4× APS was then dispensed and merged with the sample droplet. With the beads immobilized, one droplet was then split off from the sample, transported to the detector, and merged with a single-droplet containing ATP sulfurylase, luciferase, and luciferin. Photon counts were collected from the PMT every quarter second for 30 s giving 120 data points for each detection cycle. While this droplet was being detected and then transported to waste, the remaining sample (∼350 nL) containing the beads was simultaneously washed at the magnet. For this protocol, the cycle time between nucleotide additions was approximately 2.5 min which comprised 54 s for bead washing, 10 s for the nucleotide incorporation reaction, 18 s for bead collection on the magnet and preparation for washing, 38 s for droplet transport, and 30 s for reagent mixing and detection of signal.

RESULTS AND DISCUSSION

Implementation of Pyrosequencing Using Digital Microfluidics. A three-enzyme pyrosequencing protocol was adapted to digital microfluidic format and performed within submicroliter-sized droplets. A custom benchtop instrument containing control electronics, magnets, and a PMT detector was used to operate the digital microfluidic device (Figure 1B). The microfluidic cartridge consisted of a PCB containing the electrical features which was bonded with a top plate made of glass and/or plastic which contained wells for loading samples and reagents (Figure 1A). Separate wells were provided for the starting sample (template−primer duplexes bound to magnetic beads), enzyme mixtures, each of the four nucleotides, wash buffer, and waste (Figure 1C). Each of the wells was connected to an interior reservoir from which individual single-sized droplets (∼350 nL) could be dispensed on demand. A network of electrodes was arranged to form and transport droplets from each well to other locations on the cartridge including magnetic wash stations, a detection spot, and waste wells (Figure 1C). Droplets could also be merged together or split apart at various locations to initiate chemical reactions and to perform washing operations. Depending on the software program, the same cartridge was used for targeted sequencing of a known template, de novo sequencing of an unknown sample, or control reactions to check reagent and fluidic performance. A single disposable cartridge was used for each of the experiments reported here.

Reactions occurring in microfluidic volumes behave somewhat differently compared to conventional benchtop chemistry volumes. They are more significantly affected by surface interactions, especially including in this case, the interface between the aqueous droplet and the surrounding oil. Thus, the translation of pyrosequencing to the microfluidic cartridge requires

reoptimization of reagent formulations to ensure sufficient signal over background, accuracy, and read length. Luciferin, luciferase, APS, and ATP sulfurylase have an appreciable luminescent signal in the absence of pyrophosphate making reproducible detection of a single nucleotide incorporation over background a critical optimization. Extensive tests investigating pyrophosphate contamination in reagents and on the cartridge surfaces showed no appreciable contamination source; thus, any background signal was attributed to luciferin and APS serving as substrates in the luciferase reaction.[22] This effect was verified on a plate reader where the combination of ATP sulfurylase, APS, luciferin, and luciferase produced a significantly higher background signal compared to solutions containing any subset of these reagents (data not shown). The reaction was also extremely sensitive to the ratio of DNA/polymerase/dNTPs where deviation from the optimal ratio resulted in shorter and less accurate reads (data not shown). Finally, pyrosequencing was most accurate when the pyrophosphate produced from true nucleotide incorporation was within the linear range of detection by the luciferase reaction, allowing accurate detection of homopolymeric runs.

$$\mathrm{DNA}_N + \mathrm{dNTP} \xrightarrow{\text{polymerase}} \mathrm{DNA}_{N+1} + \mathrm{PPi} + \mathrm{dNDP} \quad (1)$$

$$\mathrm{PPi} + \mathrm{APS} \xrightarrow{\text{ATPsulfurylase}} \mathrm{ATP} + {\mathrm{SO_4}}^{2-} \quad (2)$$

$$\mathrm{ATP} + \mathrm{O_2} + \mathrm{luciferin} \xrightarrow{\text{luciferase}} \mathrm{AMP} + \mathrm{PPi} + \mathrm{CO_2} + \mathrm{oxyluciferase} + \mathrm{light} \quad (3)$$

The three-enzyme pyrosequencing reaction that was employed is shown above. Because pyrophosphate (PPi) is generated as a byproduct of the luciferase reaction (and apyrase is not present to degrade it), the reaction can enter a "glow" mode where the light signal persists until APS or luciferin have been exhausted. The on-cartridge reaction was optimized to generate a steady glow which was stable for up to 10 min following a single nucleotide incorporation (data not shown). In order to fully comprehend the time course of the reaction, signal was collected throughout a 60 or 30 s window, although this window could be greatly reduced without compromising the quality of the data. Immediately following detection, the magnetic beads are washed and any residual signal is eliminated along with the reaction byproduct.

An initial series of experiments was performed on the cartridge to investigate the linearity of the luminescent signal with respect to the number of nucleotides incorporated. Control experiments were performed in which combinations of dNTPs were added to primed DNA templates in solution. The addition of dNTP mixes containing one, two, or three different nucleotides gave linearly increasing signals corresponding to the incorporation of one, two, five, or eight bases as expected (Supporting Information Figure S-1). Each incorporation experiment was performed in duplicate, and excellent reproducibility was observed in all cases. Nucleotides that would not be expected to be incorporated (i.e., mismatches) served as controls and produced a background signal which was easily distinguished from true incorporations. The area under the curve (AUC) was calculated for the duplicate data sets and clearly showed a linear response over the range from one to eight bases.

Characterization of Microfluidic Washing. In the three-enzyme pyrosequencing reaction, complete removal of unincorporated or excess nucleotides at each step is critical for maintaining synchrony between the synthesized strands and is a major determinant of read length. Washing of the bead/template/primer complexes was performed by immobilizing the sample using magnetic beads, while repeatedly adding fresh buffer droplets and then removing droplets of supernatant from the sample. The magnetic bead washing steps were performed using a stationary permanent magnet embedded within the deck of the instrument. The magnetic beads were immobilized by simply transporting
the droplet containing the beads to a location situated above the magnet, and they were subsequently resuspended by transporting the droplet away from the magnet. By design, the magnetic field was strong enough to pull the beads down to the surface and permit liquid exchange for washing, but not strong enough to cause the beads to be pulled through the oil−water meniscus when the droplet was moved away. Due to the intrinsic fluid circulation within moving droplets, the beads could be completely resuspended by transporting the droplet a few electrode positions away from the magnet. A sequence of images illustrating a typical wash cycle is shown in Supporting Information Figure S-2 panels A−F.

In one experiment, this washing process was repeated 800 consecutive times and an image was captured at the end of each cycle. The images taken after 200, 400, and 799 cycles demonstrate excellent retention of beads and reproducibility of washing operations (Supporting Information Figure S-2 panels G−I). Bead retention is important for maintaining consistent signal levels throughout an experiment. However, the signal level after each successive wash cycle could also be diminished through the loss or denaturation of either the DNA template or the sequencing primer from the complex. To investigate this possibility a model system consisting of a single-stranded 81 base template coupled to magnetic beads was constructed. The template was a *Candida albicans* gDNA region located between the ITS1 and ITS2 primer binding sites (sequence in the Supporting Information), and different sequencing primers were designed to test wash efficiency (Figure 2, parts A and B), linearity of signal (Supporting Information Figure S-1), and effect of primer length and position with respect to the magnetic bead. To measure the effect of washing on the stability of the DNA/primer/bead complex, the signal produced by a single nucleotide incorporation was measured after initially washing the beads 100, 200, 400, and 800 times. Double-droplets of DNA/primer/bead complex were dispensed, transported to the magnet at position 2 (Figure 1C), and washed the indicated number of times with a double-droplet of wash buffer. The template droplets were then transported to the detector where they merged with an enzyme droplet and a complementary dNTP droplet and detected for 30 s (Figure 2A). Analyzing the AUC for each wash condition showed nearly equivalent signal for a one-nucleotide incorporation indicating little to no loss of beads, DNA, or primers. Background readings were taken using unconjugated beads without DNA which were not washed.

To determine the minimum number of wash cycles required between nucleotide incorporations, the luminescent signal was measured after each one of 10 wash steps following the incorporation of a nucleotide (Figure 2B). A droplet containing DNA/primer/bead complexes was merged with one droplet containing complementary dNTPs and one droplet containing enzymes to generate a single nucleotide incorporation. The reaction droplet was split into a single droplet prior to the addition of a double wash droplet. The signal was measured during each wash cycle for a total of 10 washes, each cycle taking

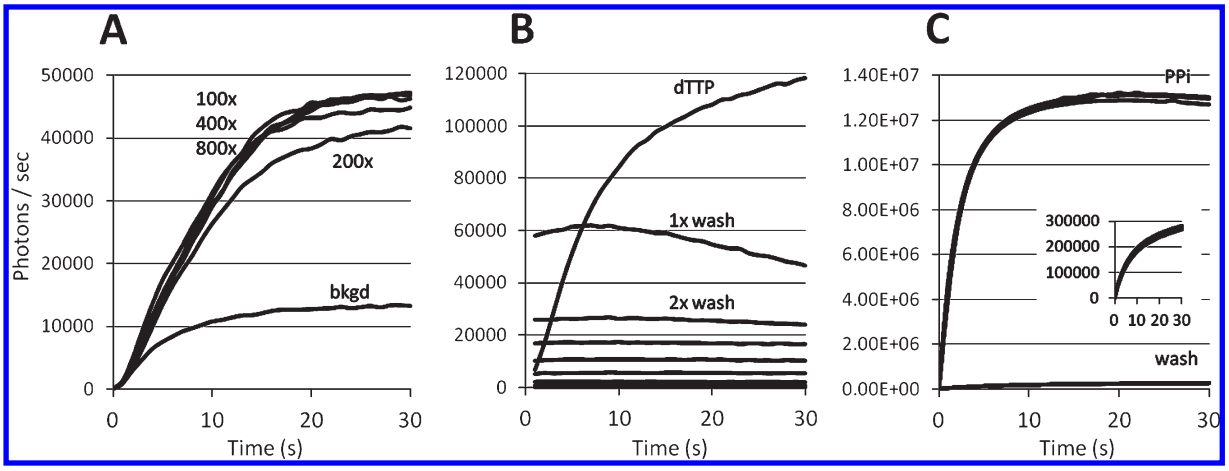

Figure 2. Characterization of signal loss (A), wash efficiency (B), and pyrophosphate carryover (C). Variable DNA inputs of a synthetic template ranging from 150 to 460 fmol were used in these experiments. (A) DNA/primer/bead complexes were washed 100, 200, 400, and 800 times prior to incorporation of dTTP. There is little difference in signal intensity indicating minimal DNA, primer, or bead loss. Background signal was collected from beads that were not conjugated with DNA. (B) After incorporation of a dTTP, residual signal was determined during each of 10 wash cycles. Six wash steps were sufficient to attain background signal levels. (C) Alternating high-concentration pyrophosphate (PPi) and wash droplets were passed under the detector and show no change in background signal suggesting no surface fouling. The inset shows wash signal on the appropriate scale for five separate droplets. The high pyrophosphate concentration was approximately 40 times greater than the expected concentration of pyrophosphate generated from a single nucleotide incorporation.

approximately 1 min. The luminescent signal decreased with each successive wash such that after six wash cycles the residual signal was equivalent to background. A control experiment in which the light output following a triple nucleotide incorporation was monitored without washing showed steady signal levels out to 10 min (data not shown) indicating that the observed decay is entirely due to washing rather than natural signal decay. With six wash cycles between each nucleotide addition, 133 cycles of nucleotide addition could be performed using the 800 wash cycles characterized above.

In order to assess the effect of carryover between samples, an alternating series of droplets containing enzymes and either pyrophosphate or wash buffer were transported through the detection spot. Significant levels of carryover of pyrophosphate into the wash buffer droplets would be detected as an elevated background signal in these experiments. One droplet of 6 pmol of pyrophosphate was dispensed and transported to the detector where it was merged with a reagent droplet containing APS, ATP sulfurylase, luciferase, and luciferin. Subsequently one droplet of wash buffer was dispensed, transported to the detector, and merged with another identical reagent droplet. This sequence was repeated five times. Each successive wash droplet produced signal levels equivalent to background demonstrating that carryover between samples at the detection spot is not significant (Figure 2C). The concentration of pyrophosphate used in these experiments was approximately 40 times greater than that which would be produced by a single-base nucleotide incorporation; thus, carryover should be manageable even for long homopolymers.

Detection of Pyrophosphate Signal. The pyrophosphate detection chemistry was optimized separately from nucleotide incorporation to ensure reproducible luminescence over extended read lengths. Droplets containing different concentrations of pyrophosphate were dispensed and mixed with a reagent droplet containing APS, ATP sulfurylase, luciferase, and luciferin at the detector. The four different pyrophosphate concentrations were selected to be roughly equivalent to the pyrophosphate generated from the incorporation of one, two, three, or four nucleotides in the full pyrosequencing reaction (Figure 3A, raw data shown in Supporting Information Figure S-3). There was little variability in signal at each pyrophosphate concentration for 36 detection cycles suggesting that the pyrophosphate detection chemistry was stable and repeatable over these lengths.

The signal measured for different pyrophosphate concentrations also enabled a standard curve to be generated. The signal produced by a single nucleotide incorporation in the full pyrosequencing reaction can be compared to the pyrophosphate standard curve to give an estimate of the amount of functional template bound to the magnetic beads. The concentration of PCR product, efficiency of conjugation to the magnetic bead, and primer hybridization are all variables which can affect the amount of template available in the pyrosequencing reaction.

DNA Sequencing. In de novo sequencing applications the four nucleotides are typically added in a repeated cyclical fashion which results in an average of about one incorporation event per every two nucleotide additions and an average of about 2.7 bases of sequence per every four nucleotide additions. In resequencing applications the nucleotides may be added in a predetermined nonrepetitive order which anticipates the actual sequence of the template and results in an incorporation event for nearly every nucleotide addition. Due to its flexibility the digital microfluidic device is compatible with either approach and can also deliver independent sequences of nucleotides simultaneously to multiple samples or adjust the nucleotide sequence in real time based on instantaneous results. As shown in Figure 3, parts B and C, both approaches were used to sequence the same template and produced similar results.

DNA samples were prepared by amplifying the ITS1 region of *C. parapsilosis* and performing template preparation steps on the bench prior to loading samples onto the cartridge. Approximately 150 fmol of DNA/primer/bead complexes were dispensed and transported to the detector where they were washed prior to the addition of the first nucleotide (described in detail in the Experimental Section). The DNA complex was merged with a

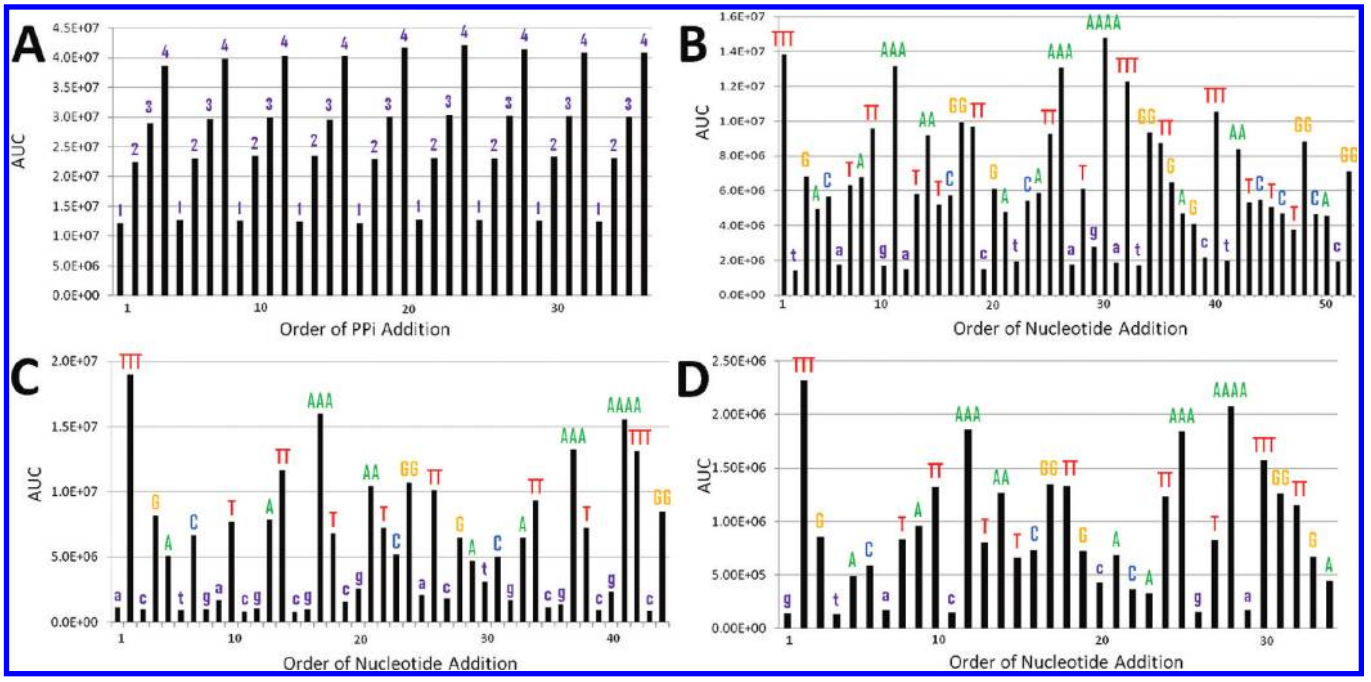

Figure 3. Reproducibility of pyrophosphate detection (A), raw pyrograms from pyrophosphate detection (B), de novo sequencing (C), and "split" protocol resequencing (D) using the same *C. parapsilosis* template. (A) AUC (photons) for sequential detections of different concentrations of pyrophosphate. Numbers indicate the homopolymer length which is approximately equivalent to the amount of pyrophosphate in the reaction. (B) Pyrogram (AUC) showing 52 cycles of nucleotide addition using a targeted resequencing protocol which included periodic mismatches to evaluate background signals. The nucleotide that was added is indicated by the letter above each bar with uppercase letters indicating expected incorporations and lowercase letters indicating expected mismatches based on the known sequence. A 62 bp sequence can be accurately read from the pyrogram by assigning a threshold level for each number of nucleotide incorporations: TTTGA^{5}CTATT^{10}AAATA^{15}ATCGG^{20}TTGAC^{25}ATTAA^{30}ATAAA^{35}ATTTG^{40}GTTGA^{45}GTTTA^{50}ATCTC^{55}TGGCA^{60}GG. (C) Pyrogram (AUC) showing 44 cycles of nucleotide addition for the same template using a de novo pyrosequencing protocol in which the four bases were repeatedly cycled in the same order. (D) Pyrogram (AUC) showing 34 cycles of nucleotide addition for the same template using a resequencing protocol in which the synthesis and detection reactions were performed in separate droplets at different times and locations on the cartridge.

dNTP droplet and an enzyme droplet, and the luminescent signal was detected continuously for 60 s. The signal measured by the detector was variable during the first 30 s because the droplet was moving with respect to the detector as it was being mixed (Supporting Information Figure S-3E). However, calculating the AUC removed this variability and enabled a single luminescence value to be determined and plotted for each nucleotide. Nucleotides that were not expected to incorporate (i.e., mismatches) were used to determine the background signal between true incorporations. The experimentally determined sequence (listed in the Figure 3 legend) was read directly from the pyrogram by assigning threshold values for the number of incorporated nucleotides. Background signals were not subtracted from the data to highlight the significant difference in signal intensity between a true nucleotide incorporation and background. Even without any signal processing, the raw data presented here easily enables 100% accurate sequence determination of 62 bases (verified by dideoxy sequencing; data not shown).

The sequence consisted of 23 single, 10 double, 5 triple, and 1 quadruple nucleotide incorporations, and 13 mismatches (i.e., background). An average AUC was determined from all single, double, and triple nucleotide incorporations and fit to a linear equation with an R^2 value of 0.9891. The signal decay was determined by plotting the AUC for each single-nucleotide incorporation versus nucleotide position and then calculating the slope and intercept of the linear fit (data not shown). Dividing the slope by the intercept and multiplying by 100 gives the decrease in efficiency over the 62 nucleotide sequence read. Single, double, and triple nucleotide signals decay by approximately 0.5% per cycle suggesting that the cycle efficiency is greater than 99.5%.

To simulate a de novo sequencing application, the previous experiment was repeated with each of the four nucleotides added in a fixed cyclical order rather than in an order which anticipated the actual sequence. Nine cycles of dATPαS, dTTP, dCTP, and dGTP were added to the DNA/primer/bead complex resulting in a 41 bp read. As before, the AUC for the entire 60 s detection was plotted against each nucleotide addition (Figure 3C, raw data shown in Supporting Information Figure S-3). The experimentally determined sequence read directly from the raw data was 100% accurate. De novo sequencing presents the DNA/primer/bead complex with many cycles of noncomplementary nucleotides over the course of a run and may require further optimization of wash protocols to prevent unwanted incorporation events. The sequence contained 13 single, 6 double, 4 triple, and 1 quadruple nucleotide incorporations as well as 20 mismatches. The average AUC for single, double, and triple nucleotide incorporations was fit to a linear curve with an R^2 value of 0.9114. It has been observed that the first successful incorporation often produces an elevated signal. Removing the first TTT incorporation from the calculation results in an R^2 value of 0.9673 which is more representative of the subsequent data.

Separation of Base Incorporation and Signal Detection Reactions. One of the key advantages of digital microfluidics is

the flexibility and control provided by independent manipulation of each droplet. This flexibility can be applied to implement a wide variety of complex protocols which may provide advantages in terms of throughput, time-to-result, or sequence fidelity. Most existing pyrosequencing approaches use a single-pot protocol where all of the enzymatic steps are performed in a single volume of liquid. Although this simplifies the fluidic operation of the device, it also means that each of the enzymatic steps must occur within a common buffer system and that the kinetics of each of the enzymatic reactions are coupled. Protocols were designed to enable the nucleotide incorporation and signal detection steps to be decoupled and performed at different times and at different locations on the cartridge. One of the advantages of this decoupling strategy is that the reaction conditions can be separately optimized for each enzymatic step. Decoupling also enables separation of the reactions in time and space so that operations can be pipelined to increase efficiency and throughput. For example, beads can be washed while reaction products are detected in separate droplets which could also be temporarily stored or queued up for detection.

Using the same microfluidic cartridge, the reagents and fluidic protocols were reformulated to decouple pyrophosphate generation from ATP generation. The magnet within the instrument was relocated to the center of the cartridge such that bead immobilization no longer occurred under the detector (magnet position 2, Figure 1C). Droplets containing DNA/primer/bead complexes were dispensed and mixed with droplets of dNTP mix containing Klenow (exo-) (described in detail in the Experimental Section). The beads were immobilized and the reaction droplet was split such that a single droplet of supernatant was removed and transported to the detector while a single droplet containing the bead complexes remained at the magnet. The droplet at the detector was merged with a reagent droplet containing luciferase, luciferin, and ATP sulfurylase, while the other droplet containing the beads was simultaneously washed. Compared to the single-pot protocol, this results in one-half of the amount of pyrophosphate which is ultimately detected because half of the supernatant remains with the beads and is subsequently washed away. The split protocol is faster than the single-pot protocol because the washing and detection operations can be performed simultaneously rather than successively. Signal collection was also reduced to 30 s, and could be further reduced to less than a second if detected within the plateau phase (raw data shown in Supporting Information Figure S-3). Feasibility of the split pyrosequencing protocol was demonstrated on the same cartridge using the *C. parapsilosis* template. The AUC was calculated and plotted for each nucleotide up to 45 bases with clear differentiation between single, double, triple, and quadruple nucleotide incorporations (Figure 3D). An average AUC was determined and fit to a linear equation with an R^2 value of 0.9516 (removing first TTT, R^2 value = 0.9799). A single background reading for dCTP in the 20th nucleotide cycle was higher than expected possibly due to asynchronous template extension.

CONCLUSIONS

The feasibility of using electrowetting-based digital microfluidics to sequence DNA by pyrosequencing has been demonstrated in this report. Although the overall sequencing through put was limited in this initial proof of concept, much higher throughputs eventually could be attained. The sequencing throughput of the device is determined by the cycle time (per nucleotide addition), the number of simultaneous sequencing reactions, the average number of bases incorporated each cycle, and the average read length. The cycle time could be substantially reduced in the future through optimization of the reaction kinetics, minimization of the detection time, further optimization of bead washing, and architectural and operational improvements to the microfluidics. It is worth noting that the generic cartridge used in these experiments was originally designed for a different application (i.e., multiplex immunoassays) and that a pyrosequencing specific design could incorporate many significant improvements including improved architectures for pipelining operations and improved well designs for managing reagents. Scaling down of electrode (and droplet) sizes would enable higher throughput and result in significantly reduced cycle times because the operating frequency of the system clock can be scaled inversely with linear dimension[5] and the reaction and diffusion kinetics are also improved at reduced length scales. The amount of light detected from the on-cartridge reaction exceeded the dark count of the PMT detector (<20 photons/s) by several orders of magnitude, even with the pinhole aperture inserted into the light path, which indicates that the system has sufficient sensitivity to scale to much smaller reaction volumes. The initial feasibility of adapting digital microfluidic pyrosequencing to picoliter scale was recently demonstrated by Welch et al.[23] Similar to Moore's law in microelectronics, scaling down of feature sizes would enable a higher density of reactions, faster operation, and reduced fabrication cost per device.

All currently available next-generation sequencing technologies achieve high levels of throughput by parallelizing thousands to millions of solid-phase reactions within a single flow cell or liquid compartment. As a result, the cost and time required to generate 100 bp or 100 million bp of sequence on most of these systems is essentially the same. Although barcoding strategies can be used to reduce the sequencing cost per sample this adds substantially to the upfront costs of sample preparation and library construction. The use of droplets as individualized flow cells to direct small amounts of reagents exactly where and when they are needed provides much greater flexibility to adapt the throughput, cost, or run time for the needs of a particular application. Certain clinical applications only require a relatively small amount of sequence, but ideally provided at a low cost per run and with a rapid turnaround time. For example, Borman et al.[24] recently demonstrated that sequencing as few as 35 base pairs of sequence located within the ITS2 region was sufficient to correctly identify over 40 different pathogenic yeasts. The implementation of pyrosequencing described here offers significant advantages in terms of instrument size, complexity, and cost, disposable cost, and achievable levels of functional integration. Because fluid control is achieved using electrical switches instead of pumps or valves the instrument can be made relatively compact and inexpensive—even portable if needed. The disposable cartridge consists of a PCB and injection-molded plastic top plate providing a low-cost consumable which, combined with the reagent savings made possible by microfluidics, enables a very low cost per run—even if the cost per sequenced base is high compared to other technologies. Finally, the broad and flexible capabilities of digital microfluidics enables the potential combination of DNA sequencing with upstream processes such as PCR, sample preparation, or cell-based manipulations within a single integrated device.

ASSOCIATED CONTENT

Supporting Information. Additional information as noted in text. This material is available free of charge via the Internet at http://pubs.acs.org.

AUTHOR INFORMATION

Corresponding Author
*E-mail: mpollack@liquid-logic.com.

ACKNOWLEDGMENT

This work was supported by a National Human Genome Research Institute (NHGRI) Grant award (R01 HG004354). The authors thank Wiley Schell, Duke University, for providing purified *C. parapsilosis* genomic DNA and thank the many other employees of Advanced Liquid Logic who contributed to the development of the platform used in these studies.

REFERENCES

(1) Schloss, J. A. *Nat. Biotechnol.* **2008**, *26*, 1113–1115.
(2) Fair, R. B. *Microfluid. Nanofluid.* **2007**, *3*, 245–281.
(3) Pollack, M. G.; Fair, R. B.; Shenderov, A. D. *Appl. Phys. Lett.* **2000**, *77*, 1725.
(4) Mugele, F.; Baret, J.-C. *J. Phys.: Condens. Matter* **2005**, *17*, R705–R774.
(5) Pollack, M. G.; Shenderov, A. D.; Fair, R. B. *Lab Chip* **2002**, *2*, 96–101.
(6) Cho, S. K.; Moon, H.; Kim, C. J. *J. Microelectromech. Syst.* **2003**, *12*, 70–80.
(7) Hua, Z.; Rouse, J. L.; Eckhardt, A. E.; Srinivasan, V.; Pamula, V. K.; Schell, W. A.; Benton, J. L.; Mitchell, T. G.; Pollack, M. G. *Anal. Chem.* **2010**, *82*, 2310–2316.
(8) Sista, R. S.; Eckhardt, A. E.; Srinivasan, V.; Pollack, M. G.; Palanki, S.; Pamula, V. K. *Lab Chip* **2008**, *8*, 2188–2196.
(9) Srinivasan, V.; Pamula, V. K.; Fair, R. B. *Lab Chip* **2004**, *4*, 310–315.
(10) Barbulovic-Nad, I.; Au, S. H.; Wheeler, A. R. *Lab Chip* **2010**, *10*, 1536–1542.
(11) Moon, H.; Wheeler, A. R.; Garrell, R. L.; Loo, J. A.; Kim, C. J. *Lab Chip* **2006**, *6*, 1213–1219.
(12) Fair, R. B.; Khlystov, A.; Tailor, T. D.; Ivanov, V.; Evans, R. D.; Pollack, M. G.; Griffin, P. B.; Zhou, J. *IEEE Des. Test Comput.* **2007**, 10–24.
(13) Jebrail, M. J.; Wheeler, A. R. *Curr. Opin. Chem. Biol.* **2010**, *14*, 574–581.
(14) Pollack, M. G.; Pamula, V. K.; Srinivasan, V.; Eckhardt, A. E. *Expert Rev. Mol. Diagn.* **2011**, *11*, 393–407.
(15) Ronaghi, M. *Genome Res.* **2001**, *11*, 3–11.
(16) Hyman, E. *Anal. Biochem.* **1988**, *174*, 423–436.
(17) Ronaghi, M.; Karamohamed, S.; Pettersson, B.; Uhlén, M.; Nyrén, P. *Anal. Biochem.* **1996**, *242*, 84–89.
(18) Ronaghi, M.; Uhlén, M.; Nyrén, P. *Science* **1998**, *281*, 363–365.
(19) Margulies, M.; Egholm, M.; Altman, W. E.; Attiya, S.; Bader, J. S.; Bemben, L. A.; Berka, J.; Braverman, M. S.; Chen, Y.-J.; Chen, Z.; Dewell, S. B.; Du, L.; Fierro, J. M.; Gomes, X. V.; Godwin, B. C.; He, W.; Helgesen, S.; Ho, C. H.; Irzyk, G. P.; Jando, S. C.; Alenquer, M. L. I.; Jarvie, T. P.; Jirage, K. B.; Kim, J.-B.; Knight, J. R.; Lanza, J. R.; Leamon, J. H.; Lefkowitz, S. M.; Lei, M.; Li, J.; Lohman, K. L.; Lu, H.; Makhijani, V. B.; McDade, K. E.; McKenna, M. P.; Myers, E. W.; Nickerson, E.; Nobile, J. R.; Plant, R.; Puc, B. P.; Ronan, M. T.; Roth, G. T.; Sarkis, G. J.; Simons, J. F.; Simpson, J. W.; Srinivasan, M.; Tartaro, K. R.; Tomasz, A.; Vogt, K. A.; Volkmer, G. A.; Wang, S. H.; Wang, Y.; Weiner, M. P.; Yu, P.; Begley, R. F.; Rothberg, J. M. *Nature* **2005**, *437*, 376–380.
(20) Zhou, G.; Kamahori, M.; Okano, K.; Harada, K.; Kambara, H. *Electrophoresis* **2001**, *22*, 3497–3504.
(21) Russom, A.; Tooke, N.; Andersson, H.; Stemme, G. *Anal. Chem.* **2005**, *77*, 7505–7511.
(22) Nyrén, P.; Lundin, A. *Anal. Biochem.* **1985**, *151*, 504–509.
(23) Welch, E. R. F.; Lin, Y.-Y.; Madison, A.; Fair, R. B. *Biotechnol. J.* **2011**, *6*, 165–176.
(24) Borman, A. M.; Linton, C. J.; Oliver, D.; Palmer, M. D.; Szekely, A.; Johnson, E. M. *J. Clin. Microbiol.* **2010**, *48*, 3648–3653.